J. Univ. Kuwait (Sci.) **9**, 1982

Pressure distribution around a laterally loaded pile

MOSAID M. AL-HUSSAINI

Department of Civil Engineering, University of Kuwait

ABSTRACT

In this study a closed form solution is derived for the determination of stress distribution in soil surrounding a laterally loaded pile. The solution is presented in the form of influence charts to enable quick and easy determination of normal and shear stresses induced by the lateral thrust acting on the pile. Comparison is made between normal stresses obtained from this study and those obtained under an infinite strip loaded with uniform pressure. The theoretical analysis showed that the geometry of the pile surface greatly influenced the pressure distribution within the surrounding soil.

INTRODUCTION

Piles are often subjected to lateral forces arising from such effects as winds on the associated superstructure, centrifugal acceleration of vehicles moving over bridges with longitudinal curvature, drag and inertia forces induced by water flowing around bridge piers. The procedure for determining the lateral load-deflection behaviour of piles is based on the analysis of the well-known differential equation of beam on an elastic foundation (Hetenyi 1946; Matlock & Reese 1960; Reese & Welch 1975), i.e.,

$$E\,I(d^4y)/(dz^4) - P = 0 \qquad (1)$$

$$P = E_s y$$

where E = modulus of elasticity of the pile, I = moment of inertia of the pile cross section, P = lateral soil reaction per unit length, z = vertical distance along the axis of the pile, y = lateral deflection of the pile, and E_s = soil modulus.

A lateral load applied to the top of a pile is transferred to the surrounding soil as illustrated in Fig. 1. Before any lateral load is applied to the pile, the pressure distribution on the pile will be similar to that shown in Fig. 1b. Under this condition, it follows that the resultant force on the pile obtained by integrating the pressure around a section is zero. If, however, the pile is given a lateral deflection y at depth L from the ground surface, the pressure distribution at that section will be similar to that displayed in Fig. 1c. In this case, the integration of the pressure distribution around the section will yield a resultant force, P_1, per unit length of the pile.

Comparing the two pressure distributions shown in Fig. 1b and c, it is reasonable to

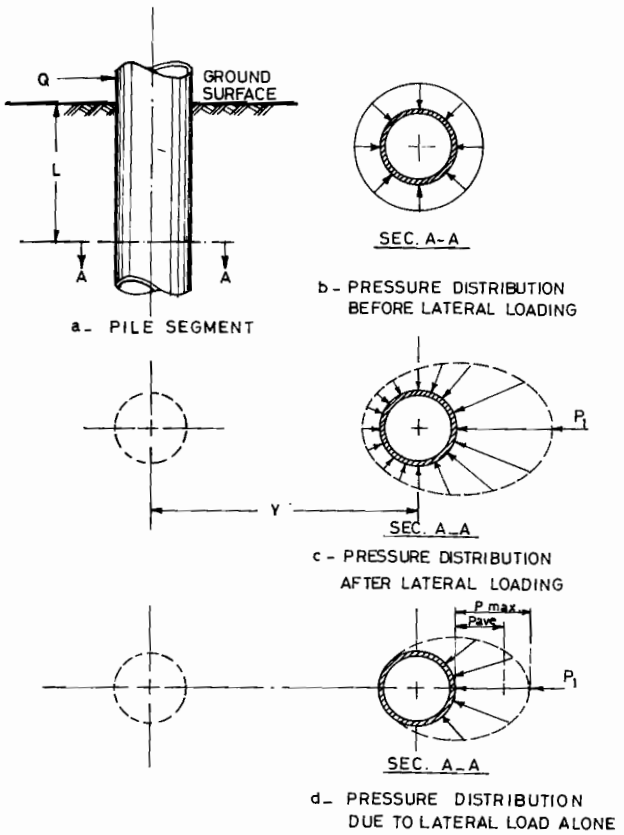

Fig. 1. Schematic pressure distribution around laterally loaded pile.

assume that the pressure distribution presented in Fig. 1c consists of two parts. The first is a uniformly distributed pressure, similar to that shown in Fig. 1b, resulting from the lateral pressure of the soil, and the other is due to the effect of lateral thrust of the pile as shown in Fig. 1d. It is seen then that the integration of pressure around the section under this assumption will also yield a resulting force, P_1, per unit length of the pile.

Although several methods have been proposed for the design of laterally loaded piles (Broms 1964; Poulos 1971; Frank 1973; Reese & Welch 1975), the particular approach used by the petroleum industry and by many investigators (Matlock & Reese 1960; Reese & Welch 1975; Ismael & Klym 1978), makes use of a pressure-deflection relationship called $P-y$ curves of piles originally proposed by McClelland & Focht (1958). The procedure for obtaining experimentally the $P-y$ curves involves the field testing of an instrumented pile where the bending moment (M_z) along the pile length can be obtained. From strain measurements the appropriate expression of the bending moment obtained in this manner can be used subsequently for determining P by solving

$$P = (d^2M_z)/(dz^2) \tag{2}$$

The solution of Eqn (2) is carried out numerically with appropriate boundary conditions.

The criteria used in the design for stiff clay (Reese & Welch 1975) can be used in a dimensionless ratio P/P_u where P_u is the ultimate lateral resistance of the soil at depth of interest. Dimensionally, P_u is expressed as force/(length^2), while the lateral soil reaction on the pile is expressed as force/length. Thus, to make P/P_u a dimensionless ratio it has been suggested (Matlock & Reese 1960) that the ultimate resistance of soft clay be expressed as

$$P_u = cN_cD \tag{3}$$

where c = average shear strength at depth L, N_c = bearing capacity factor, and D = pile diameter.

Since the ultimate bearing capacity of soft clay $q_u = 9c$, by setting $P_u = q_uD$, the dimensionless ratio (P/P_u) can be expressed in the form

$$\frac{P}{P_u} = \frac{P}{q_uD} = \frac{(P/D)}{q_u} = \frac{P_{ave}}{q_u} \tag{4}$$

where P_{ave} = average lateral soil reaction across the pile width.

Considering Fig. 1d now, it can be seen that the average pressure P_{ave} is less than the maximum pressure P_{max}. If the difference between these pressures is significant, then the design criteria based on the $P-y$ curves require some modification. Thus the objective is to establish a relationship between P_{ave}, which is used in $P-y$ curves, and the maximum lateral soil pressure, P_{max}, around laterally loaded piles.

THEORETICAL CONSIDERATION

A theoretical solution for predicting the stress distribution around a segment of pile as shown in Fig. 1d is extremely difficult since it is a three-dimensional problem and the

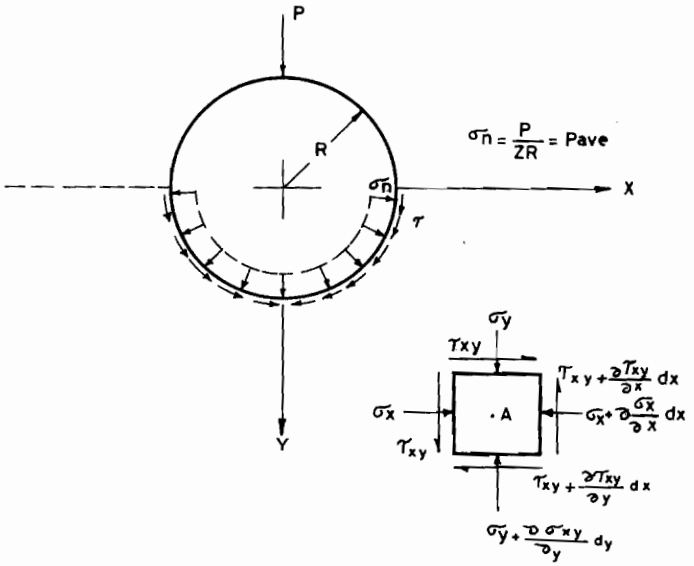

Fig. 2. Stresses at a point in the neighbourhood of a pile.

behaviour of natural soil around a pile is not well understood. However, if we consider the state of stress around the pile to be planer, and the soil media as homogeneous and isotropic, then a closed form solution similar to the one developed by Al-Hussaini & Gilbert (1974) for stress distribution beneath a rigid wheel can be generated.

Consider a segment of the pile as shown in Fig. 1d, under a normal stress, σ_n, and a shear stress, τ, acting along the contact surface of the pile resulting from the lateral thrust of the pile (Q) on the soil as shown in Fig. 2. To guarantee the uniqueness of the solution, the conditions relevant to equilibrium, boundaries and compatibility must be satisfied. Using the usual nomenclature, the equilibrium conditions for an element A within the soil surrounding the pile can be satisfied by the following harmonic differential equation

$$\nabla^2(\sigma_x+\sigma_y) = \nabla^4[U(x,y)] \tag{5}$$

where σ_x, σ_y are the normal stresses acting on the x and y planes, respectively, ∇^2 is the Laplacian operator and $U(x,y)$ is a stress function which is related to the normal and shear stresses as follows:

$$\sigma_x = \frac{\partial^2 U(x,y)}{\partial y^2} \tag{6a}$$

$$\sigma_y = \frac{\partial^2 U(x,y)}{\partial x^2} \tag{6b}$$

$$\tau_{xy} = \frac{\partial^2 U(x,y)}{\partial x \partial y} \tag{6c}$$

where τ_{xy} is the shear stress acting on plane bounded by the x and y axes. The solution of Eqn (5) is obtained easily by using complex variables following a procedure presented by Timoshenko & Goodier (1962) to obtain the following:

$$U(x,y) = 1/2[\bar{z}\phi(z)+z\overline{\phi(z)}+\chi(z)+\overline{\chi(z)}] \tag{7}$$

where $\phi(z)$ and $\chi(z)$ are analytic functions, and $\overline{\phi(z)}$ and $\overline{\chi(z)}$ are their complex conjugates which can be determined from the approximate boundary conditions. It has been shown (Timoshenko & Goodier 1962) that shear and normal stresses can be expressed as

$$\sigma_x+i\tau_{xy} = \phi'(z)+\overline{\phi'(z)}-z\overline{\phi''(z)}-\overline{\chi''(z)} \tag{8a}$$

$$\sigma_y-i\tau_{xy} = \phi'(z)+\overline{\phi'(z)}+z\overline{\phi''(z)}+\overline{\chi''(z)} \tag{8b}$$

By substituting $\phi'(z)$, $\chi''(z)$ for $\Phi(z)$ and $\Psi(z)$ respectively and subsequently adding and substracting Eqns (8a) and (8b), the following expressions may be obtained:

$$\sigma_x+\sigma_y = 2[\Phi(z)+\overline{\Phi(z)}] = 4\mathrm{Re}[\Phi(z)] \tag{9a}$$

$$\sigma_y-\sigma_x+2i\tau_{xy} = 2[\bar{z}\Phi'(z)+\Psi(z)] \tag{9b}$$

REPRESENTATION OF STRESSES IN CURVILINEAR COORDINATES

Eqn (9) gives the Cartesian components of stress in terms of complex potentials $\Phi(z)$ and $\Psi(z)$. Since the region under consideration contains curved boundary, it is more convenient to define z as a function of t in curvilinear coordinates such that

$$z = f(t) = f(r+is) \tag{10}$$

where r and s represent the curvilinear coordinates in the t-plane. It is also necessary to transform the functions $\Phi(z)$ and $\Psi(z)$ from the z-plane to a corresponding one in the t-plane, using the following relationships:

$$\Phi(z) = \Phi[f(t)] = \Phi(t) \tag{11a}$$

$$\Psi(z) = \Psi[f(t)] = \Psi(t) \tag{11b}$$

The corresponding transformation of Cartesian stress components, following the procedure presented by Timoshenko & Goodier (1962) gives

$$\sigma_s - \sigma_r + 2i\tau_{rs} = (\sigma_x - \sigma_y + 2i\tau_{xy})e^{2i\theta} \tag{12a}$$

and

$$\sigma_r + \sigma_s = \sigma_x + \sigma_y \tag{12b}$$

where

$$e^{2i\theta} = f'(t)/\overline{f'(t)} \tag{12c}$$

Assuming σ_n and τ be the normal and shear stresses, respectively applied at the boundary B in the z-plane, as shown in Fig. 2, then

$$(\sigma_n + i\tau)_B = (\sigma_y + i\tau_{xy})_B = \left[\frac{\sigma_x+\sigma_y}{2} + \frac{\sigma_y-\sigma_x+2i\tau_{xy}}{2}\right]_B \tag{13}$$

By the substitution of Eqns (9), (11) and (12), Eqn (13) can be rewritten as

$$(\sigma_n + i\tau)_B = \{\Phi(t) + \overline{\Phi(t)} + \overline{f(t)}\,[\Phi'(t)/f'(t)] + \Psi(t)\,[f'(t)/\overline{f'(t)}]\}_B \tag{14}$$

Because the boundary of the region under consideration in the z-plane, shown in Figs 2 and 3, corresponds only to the real axis of the t-plane (i.e. $s=0$ and $t=r$) the stress expressed by Eqn (14) reduces along this boundary to

$$\sigma_n + i\tau = \overline{\Phi(r)} + \Phi(r) + \overline{f(r)}\,[\Phi'(r)/\overline{f'(r)}] + \Psi(r)\,[f'(r)/\overline{f'(r)}] \tag{15}$$

whose conjugate is

$$\sigma_n - i\tau = \Phi(r) + \overline{\Phi(r)} + f(r)\,[\overline{\Phi'(r)}/f'(r)] + \overline{\Psi(r)}\,[\overline{f'(r)}/f'(r)] \tag{16}$$

DETERMINATION OF STRESS DISTRIBUTION

The determination of stresses around the pile section shown in Fig. 2 requires a function which can map the region containing the circular boundary of the pile and the surrounding soil, represented by the z-plane on to a semi-infinite plane representing the

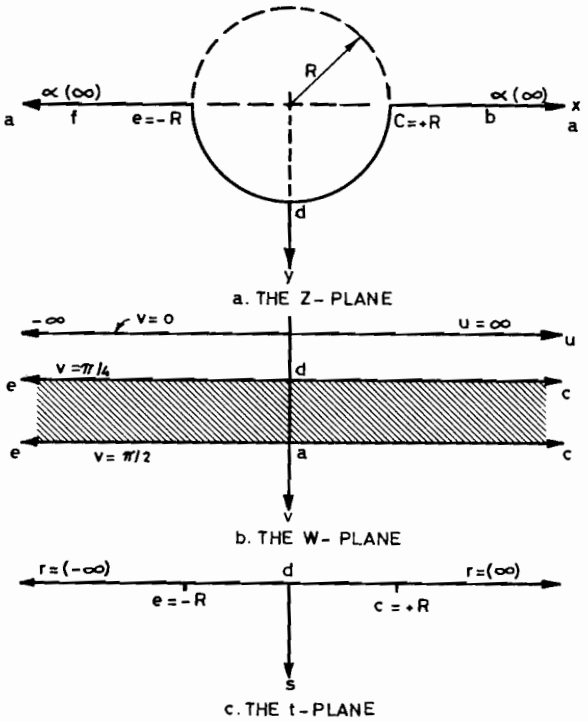

Fig. 3. Transformation of half space with semi-circle on to half space.

t-plane, as shown in Fig. 3. This is accomplished by mapping the z-plane on to an auxiliary plane, called w-plane, using the following function:

$$z = R \tanh(w) \tag{17}$$

Using the Schwarz–Christoffel transformation (Churchill 1974) to map the w-plane on to the t-plane, it is possible to relate the z-plane to t-plane by

$$z = R \tanh\left[\frac{\pi i}{2} - \frac{1}{4}\ln\left(\frac{t-R}{t+R}\right)\right] \tag{18}$$

Since the boundary of the t-plane, represented by half space, is bounded by a simple closed curve, and since an analytic function, represented by Eqns (15) and (16) is known on its boundary, the Cauchy integral formula (Churchill 1974) can be utilized to determine the value of a function at any point within the enclosed region, e.g.

$$H(t_0) = \oint_C \frac{H(t)}{t - t_0}\, dt \tag{19}$$

where $H(t)$ is a known function on the boundary of the simple closed curve C and $H(t_0)$ is the value associated with any point, t_0, in the interior of the boundary.

Referring to Eqns (15) and (14), it is seen that functions $\overline{\Phi(r)}$, $\Phi(r)$, $\overline{f(r)}$, $f(r)$, and $\Psi(r)$ represent the boundary values of $\overline{\Phi(t)}$, $\Phi(t)$, $f(t)$, $\overline{f(t)}$, and $\Psi(t)$, respectively.

Since all of these boundary values vanish at infinity it follows that the preceeding Cauchy integral formula can be applied in this case.

Since the boundary stresses σ_n and τ act only in the interval $-R \leq r \leq +R$ then the functions $\Phi(t)$, $\Phi'(t)$ and $\Psi(t)$ can be obtained after using Eqn (19) and assuming τ to be negligible, as

$$\Phi(t) = \frac{\sigma_n}{2\pi i} \ln\left(\frac{t-R}{t+R}\right) \tag{20a}$$

$$\Phi'(t) = \frac{\sigma_n}{\pi i}\left(\frac{R}{t^2-R^2}\right) \tag{20b}$$

$$\Psi(t) = -\frac{G(t)\Phi(t)}{f'(t)} \tag{20c}$$

where

$$G(t) = R \tanh(w_1) \tag{20d}$$

$$w_1 = \frac{1}{3}\,\mathrm{Re}\,(w_2) + i\,\mathrm{Im}\,(w_2) \tag{20e}$$

$$w_2 = \frac{\pi i}{2} - \frac{3}{4} \ln\left(\frac{t-R}{r+R}\right) \tag{20f}$$

A more detailed derivation of Eqn (20) is presented elsewhere (Al-Hussaini & Gilbert 1974). If the functions $\Phi(t)$, $\Psi(t)$ and $G(t)$ are known, then σ_x, σ_y and τ_{xy} at any point around the pile can be determined as follows:

$$\sigma_y = 2\,\mathrm{Re}\,[\Phi(t)] + \mathrm{Re}\,\{\overline{f(t)}\,[\Phi'(t)/f'(t)] + \Psi(t)\} \tag{21a}$$

$$\sigma_x = 2\,\mathrm{Re}\,[\Phi(t)] - \mathrm{Re}\,\{\overline{f(t)}\,[\Phi(t)/f'(t)] + \Psi(t)\} \tag{21b}$$

$$\tau_{xz} = \mathrm{Im}\,\{\overline{f(t)}\,[\Phi'(t)/f'(t)] + \Psi(t)\} \tag{21c}$$

Eqn (21) can easily be programmed to obtain numerical values of σ_y, σ_x and τ_{xy} for any given normal surface stress, σ_n.

PRESENTATION OF RESULTS

The conversion of Eqn (21) into explicit algebraic expressions would result in a presentation too long and complicated to be immediately useful. To simplify the solution, however, an extensive computation was carried out and results are presented in a dimensionless form which permits an easy determination of the pattern of stresses in the affected soil around the pile. The solution is presented in the form of an influence chart where the ordinate and abscissa are normalised in terms of the pile diameter, D. Isobars of the induced stresses are given as fractions of the average applied pressure, $\sigma_n = P/D$. Isobars for σ_y, σ_x, and τ_{xy} are presented in Figs 4, 5 and 6, respectively. It might be noticed in Fig. 4 that there is a small region close to the pile surface where σ_y is larger than the average applied surface pressure.

VERIFICATION OF RESULTS

The stress distribution obtained in this investigation was compared with those

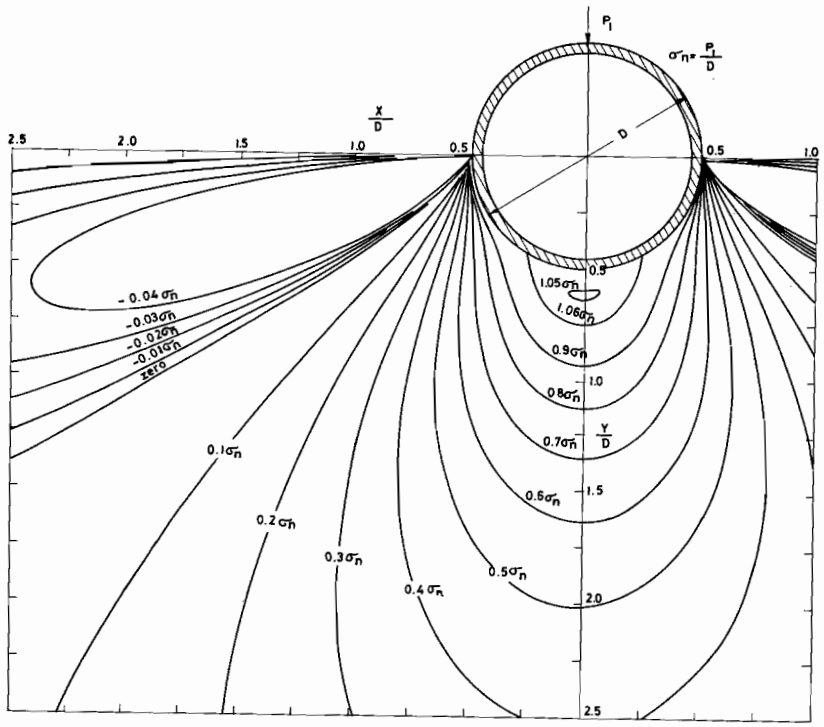

Fig. 4. Isobars of σ_y induced by radial pressure σ_n.

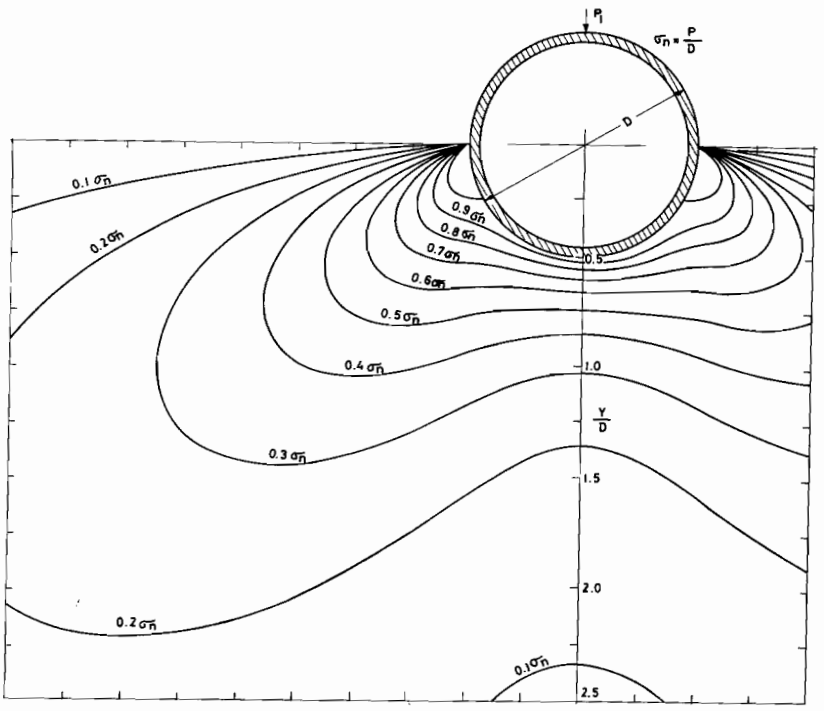

Fig. 5. Isobars of σ_x induced by radial pressure σ_n.

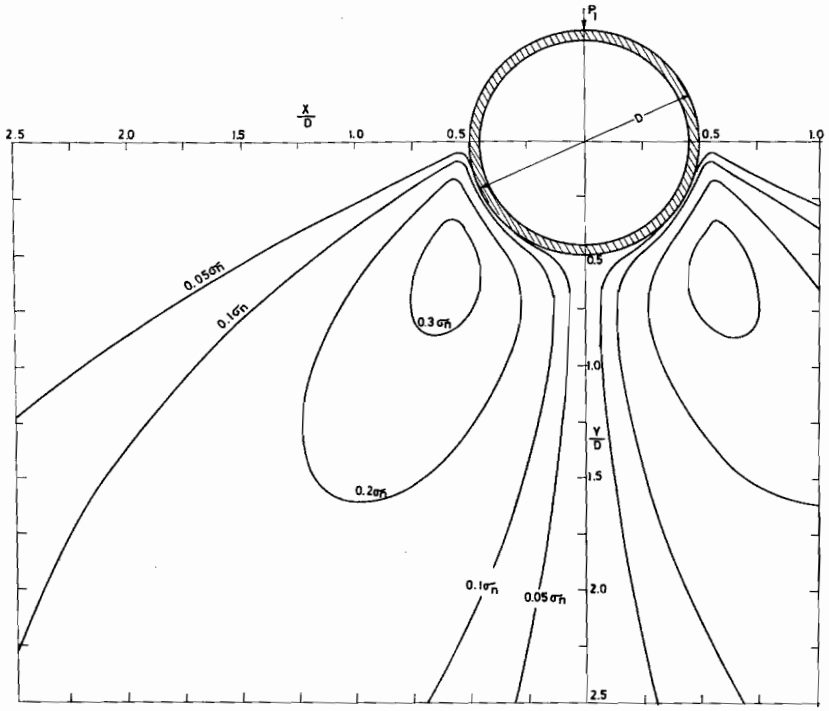

Fig. 6. Isobars of τ_{xy} induced by radial pressure σ_n.

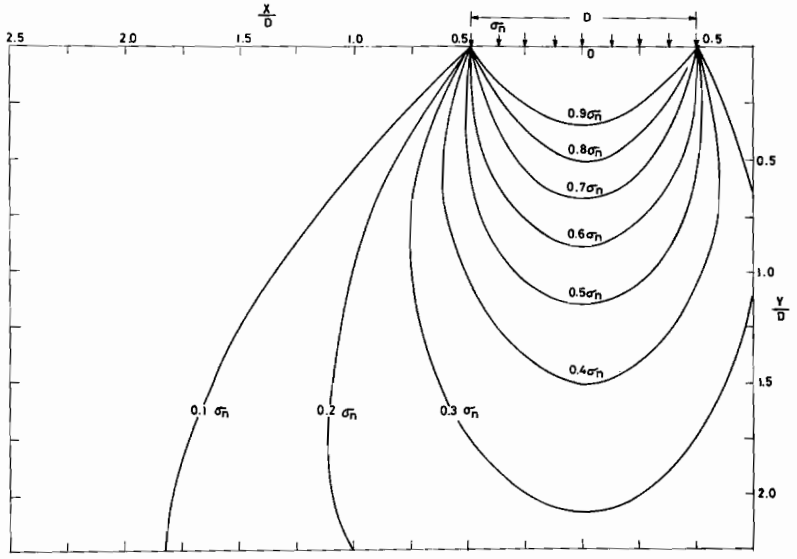

Fig. 7. Isobars of σ_y induced by uniform pressure σ_n on infinite strip.

obtained from stress beneath an infinite strip loaded with a uniform pressure using the Boussinesq theory (Sowers & Sowers 1970). The isobars of vertical stresses beneath an infinite strip with width D are presented in Fig. 7. The comparison between these and the isobars of σ_y stress obtained in this study indicates that at any distance along the ordinate the magnitude of σ_y obtained in this study is much higher than that obtained from the loaded infinite strip. This point can be explained more clearly by the following example which is based on actual field test.

Illustrative example

A 30 in (0·76 m) diameter and 44 ft (13·42 m) drilled shaft is embedded to a depth of 42 ft (12·81 m) in Beaumont Clay (Reese & Welch 1975). A lateral force of 30 tons (267 kN) applied to the top of the shaft induces a maximum lateral thrust of 0·5 ton/in (175 kN/m) at a depth of 3·13 ft (0·95 m) below the ground surface. Compute the soil pressure along the radial direction of the induced thrust and compare results with those obtained from Boussinesq solution for semi-infinite strip.

Solution

Let the diameter of the shaft be designated by D, the applied lateral force designated by Q, and the induced lateral thrust at a distance L below the ground surface designated by P_1 as shown in Fig. 1. In order to calculate the stress distribution within the soil the average contact pressure on the surface of the shaft must be determined.

$$\sigma_{ave} = \sigma_n = \frac{P_1}{D} = \frac{1000}{3} = 33{\cdot}34 \text{ psi } (230 \text{ kN/m}^2)$$

Once σ_n is calculated, then the stress σ_y along the radial direction of P_1 can be determined from Fig. 4 for the circular shaft and from Fig. 7 for the case of vertical stress along the centre of infinite strip of width D. This is accomplished by selecting radial distance Y/D and reading the corresponding contours of σ_y that pass through the selected points. Stresses for several points are presented in Table 1.

The variation of soil pressure along the radial direction of P_1 is presented

Table 1. Stresses for selected points along a circular shaft and an infinite strip

		Circular shaft		Infinite strip	
Radial distance Y (in)	Ratio Y/D	Contour reading (Fig. 4)	Radial stress σ_y (psi)	Contour reading (Fig. 7)	Vertical stress σ_y (psi)
15·0	0·50	1·00	33·34	0·82	27·34
22·5	0·75	1·04	34·68	0·65	21·67
30·0	1·00	0·86	28·64	0·55	18·34
37·5	1·25	0·75	24·98	0·46	15·34
45·0	1·50	0·65	21·65	0·40	13·34
60·0	2·00	0·50	16·65	0·31	10·33
75·0	2·50	0·42	14·00	0·25	8·34

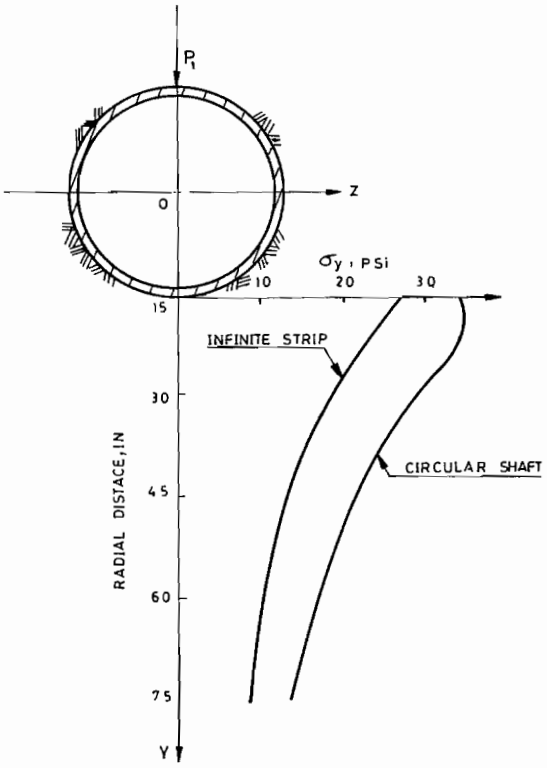

Fig. 8. Variation of soil pressure along the radial direction of the induced lateral thrust (1 in = 25·4 mm, 1 psi = 6·9 kN/m^2).

graphically in Fig. 8. This figure shows that σ_y as obtained from the infinite strip is approximately equal to two-thirds that obtained by this study.

Comparison between Fig. 4 and Fig. 7 indicates that the size of the region which has a significant σ_y (i.e. $\sigma_y > 0{\cdot}1\ \sigma_n$) is much larger around the pile than that of the loaded infinite strip. This has special significance since both short- and long-term deflection of pile under sustained loads are influenced by the intensity and distribution of σ_y.

CONCLUSION

The present study indicates that σ_y stress obtained from a loaded infinite strip is about two-thirds that obtained in this study. The study also indicates that the size of the region with significant σ_y is much larger around the pile than that of an infinite strip. The geometry of the pile should be taken into account in the analysis and design of laterally loaded pile.

REFERENCES

Al-Hussaini, M. & Gilbert, P.A. 1974. Stress and shearing resistance in soil beneath a rigid wheel. USAE, Waterways Experiment Station, TR-S-74-7.

Broms, B.B. 1964. Lateral resistance of piles in cohesive soils. J. Soil Mech. Found. Eng., ASCE **90:** SM2, 27–63.

Churchill, R.V. 1974. Complex variables and applications, pp. 129–30. McGraw-Hill, New York.

Frank, E. 1973. Principle for test loading of large-bored pile by horizontal loads. VIIIth Int. Conf. SMFE, **2.1:** 97–104.

Hetenyi, M. 1946. Beams on elastic foundation, pp. 2–6. University of Michigan Press.

Ismael, N.E. & Klym, T.W. 1978. Behaviour of rigid piers in layered cohesive soils. J. Geotech. Eng. Div. ASCE **104:** GT8, 1061–74.

Matlock, H. & Reese, L.C. 1960. Generalized solution for laterally loaded piles. J. Soil Mech. Found. Eng., ASCE **86:** SM5, Part 1, 63–91.

McClelland, B. & Focht, J.A. 1958. Soil modulus for laterally loaded piles. Trans. ASCE **123:** 1049–86.

Poulos, H.G. 1971. Behaviour of laterally loaded piles. I. Single piles. J. Soil Mech. Found. Eng., ASCE **97:** SM5, 711–32.

Reese, L.C. & Welch, R.C. 1975. Lateral loading of deep foundation in stiff clay. J. Geotech. Eng. Div. ASCE **101:** GT7, 633–48.

Sowers, G.B. & Sowers, G.F. 1970. Introductory soil mechanics and foundation, pp. 401–2. Macmillan, New York.

Timoshenko, S. & Goodier, N.J. 1962. Theory of elasticity, pp. 168–79. McGraw-Hill, New York.

(Received 21 April 1982)

توزيع الضغوط حول ركائز أساسات تحت تأثير قوى جانبية

مساعد الحسيني
قسم الهندسة المدنية بجامعة الكويت

خلاصة

لقد أوجدنا في هذا البحث حلا رياضيا لايجاد توزيع الضغوط داخل التربة المحيطة بركائز أساسات مسلط عليها ضغوط جانبية . وضع الحل الرياضي على صورة خطوط بيانية لتجعل عملية ايجاد الضغوط العمودية وضغوط القص حول ركائز الأساسات المسلط عليها قوى جانبية سريعة وسهلة . لقد أجريت مقارنة في هذا البحث بين الضغوط العمودية التي وجدناها بالحل الرياضي وتلك التي يمكن ايجادها تحت شريحة لامتناهية الطول ومسلط عليها ضغط متساو . أظهر التحليل الرياضي أن الشكل الهندسي لركائز الأساسات يؤثر تأثيرا كبيرا في توزيع الضغوط في التربة التي تحيط بها .